

Portland State University

PDXScholar

Biology Faculty Publications and Presentations

Biology

6-2019

Antioxidant Capacity and Anoxia-tolerance in *Austrofundulus limnaeus* Embryos

Josiah Tad Wagner
Portland State University

Michael J. Knapp
Portland State University

Jason E. Podrabsky
Portland State University, podrabsj@pdx.edu

Follow this and additional works at: https://pdxscholar.library.pdx.edu/bio_fac



Part of the [Biology Commons](#)

Let us know how access to this document benefits you.

Citation Details

Wagner, J. T., Knapp, M. J., & Podrabsky, J. E. (2019). Antioxidant capacity and anoxia-tolerance in *Austrofundulus limnaeus* embryos. *Journal of Experimental Biology*, jeb-204347.

This Post-Print is brought to you for free and open access. It has been accepted for inclusion in Biology Faculty Publications and Presentations by an authorized administrator of PDXScholar. Please contact us if we can make this document more accessible: pdxscholar@pdx.edu.

Antioxidant capacity and anoxia-tolerance in *Austrofundulus limnaeus* embryos

Josiah T. Wagner^{1,2}, Michael J. Knapp¹ and Jason E. Podrabsky^{1*}

1. Department of Biology, Portland State University, P.O. Box 751, Portland, OR 97207

2. Knight Cancer Institute Cancer Early Detection Advanced Research Center, Oregon Health & Science University, 3181 SW Sam Jackson Park Road, Mailcode: KR-CEDR, Portland, OR 97239

*Corresponding author:

Jason E. Podrabsky

Department of Biology

Portland State University

P.O. Box 751

Portland, OR 97207

Email: jpod@pdx.edu

Tel: 503.725.5772

Keywords: Catalase, glutathione peroxidase, superoxide dismutase, development, ORAC

Summary Statement

Embryos of *Austrofundulus limnaeus* have a remarkable tolerance of reactive oxygen species that is likely supported by a combination of small molecule antioxidants and a high activity of antioxidant enzyme systems during early development.

Abstract

Embryos of *Austrofundulus limnaeus* can tolerate extreme environmental stresses by entering into a state of metabolic and developmental arrest known as diapause. Oxidative stress is ubiquitous in aerobic organisms and the unique biology and ecology of *A. limnaeus* likely results in frequent and repeated exposures to oxidative stress during development. Antioxidant capacity of *A. limnaeus* was explored during development by measuring antioxidant capacity due to small molecules and several enzymatic antioxidant systems. Diapause II embryos can survive for several days in 1% hydrogen peroxide without indications of negative effects. Surprisingly, both small and large molecule antioxidant systems are highest during early development and may be due to maternal provisioning. Antioxidant capacity is largely invested in small molecules during early development and in enzymatic systems during late development. The switch in antioxidant mechanisms and decline in small molecule antioxidants during development correlates with the loss of extreme anoxia tolerance.

Introduction

Organisms dependent on molecular oxygen for metabolic processes will inevitably produce highly reactive intermediates such as superoxide anion (O_2^-), hydrogen peroxide (H_2O_2), and hydroxyl radical ($OH\cdot$). These molecules are common forms of reactive oxygen species (ROS), and while excessive quantities of ROS can be cytotoxic, ROS also have important functional roles such as intercellular signaling (Thannickal and Fanburg, 2000; Valko et al., 2007). During normal cellular respiration, vertebrates must maintain a constant flow of bioavailable oxygen and a balance of ROS production, retention, and removal. Because of the high aerobic metabolic demands of some organ tissues such as the heart and brain, most vertebrates are particularly vulnerable to fluctuations in oxygen availability and ROS concentration (Lutz and Nilsson, 2004; Lutz et al., 1996). If the flow of oxygen is interrupted to critical tissues, vertebrates generally suffer an increase in cytotoxic ROS production and cell death following reintroduction of oxygen to the tissues. This phenomenon has been well characterized in mammals, which have been shown to experience significant increases in ROS and neuronal death following five minutes or longer of ischemia and subsequent reperfusion (Cao et al., 1988; Kirino, 1982). However, there are several aquatic vertebrates that are unusually tolerant to extended periods of anoxia (Podrabsky et al., 2012). One of these anoxia-tolerant organisms, the Venezuelan annual killifish *Austrofundulus limnaeus* (Meyers; Cyprinodontiformes: Rivulidae) produces embryos with an overall anoxia tolerance that is approximately two orders of magnitude greater than any other examined vertebrate species (Podrabsky et al., 2007). In this investigation we explore the antioxidant capacity of this remarkable vertebrate model of anoxia tolerance.

Like other annual killifishes, *A. limnaeus* inhabits ephemeral ponds that experience seasonal or daily periods of desiccation, hypoxia, anoxia, and hyperoxia (Hrbek et al., 2005; Podrabsky et al., 1998). In order to survive these highly variable and seasonally uninhabitable

conditions, *A. limnaeus* embryos enter into a state of suspended animation and profound metabolic depression known as diapause (Podrabsky and Hand, 1999; Wourms, 1972c). Annual killifishes may enter into diapause anywhere between one and three times during embryonic development (Podrabsky et al., 2017; Wourms, 1972a; Wourms, 1972b; Wourms, 1972c). Diapause I, which occurs prior to axis formation, appears to be facultative or rare in *A. limnaeus* under laboratory conditions. Diapause II (DII) occurs approximately midway through embryonic development, and at this stage embryos have the foundations of a central nervous system, a functional tubular heart, and 38-40 pairs of somites. Finally, embryos may also arrest at diapause III (DIII), which occurs at the end of embryonic development just prior to hatching. Previous work has shown that a combination of increased molecular chaperone expression, reduced oxidative phosphorylation, accumulation of GABA, depressed protein synthesis, and inhibition of apoptosis likely all contribute to the anoxia-tolerant phenotype (Chennault and Podrabsky, 2010; Duerr and Podrabsky, 2010; Meller and Podrabsky, 2013; Podrabsky and Hand, 2000; Podrabsky et al., 2007; Podrabsky et al., 2012; Podrabsky and Somero, 2007). Yet, the likely essential mechanisms of ROS regulation in the *A. limnaeus* system have yet to be elucidated.

It is now well-known that cellular ROS regulation is essential to vertebrate survival and development (Rudneva, 2013). Generally, vertebrates manage ROS levels using primarily two mechanisms: small molecule antioxidants, and antioxidant enzymes (Matata and Elahi, 2007). The major small molecule that contributes to antioxidant capacity is thought to be the intracellular tripeptide glutathione (GSH) and its oxidized form, glutathione disulfide (Masella et al., 2005). GSH is synthesized in many vertebrate cells and depletion of GSH results in death (Meister, 1994). Vertebrates also maintain ROS homeostasis with a well-studied and elaborate array of enzyme systems. These enzymes include: superoxide dismutases (SOD's), which catalyze the conversion of O_2^- to H_2O_2 ; catalase, which catalyzes the conversion of H_2O_2 to water and molecular oxygen; and glutathione peroxidases (GPx's), which catalyze the conversion of H_2O_2 to water using GSH as a cofactor (Matata and Elahi, 2007). Both small molecule and

enzymatic antioxidant systems have been shown to be active and dynamic during normal teleost development and appear to be widely conserved among vertebrates (Drouin et al., 2011; Gerhard et al., 2000; Margis et al., 2008; Martínez-Alvarez et al., 2005; Rudneva, 2013; Zelko et al., 2002).

Currently, the extent to which anoxia-tolerant vertebrates deviate in antioxidant capacity between anoxia-sensitive and other anoxia-tolerant species is unclear. Studies in anoxia-tolerant freshwater turtles suggest that a combination of high GSH/GSSG ratios, maintenance of ascorbic acid tissue concentration during ischemia, and expression of antioxidant enzymes may all contribute to their anoxia tolerance as adults (Rice and Cammack, 1991; Storey, 1996; Storey, 2007; Willmore and Storey, 1997). Whether or not this strategy can be generalized to other anoxia-tolerant vertebrates has yet to be determined. In this work, we demonstrate the ability of embryos of *A. limnaeus* to tolerate highly oxidizing conditions by treatment with H₂O₂ and show its effect on termination of diapause. We characterize the dynamics of SOD, catalase, and GPx expression and activity during normal *A. limnaeus* embryonic development, and estimate small molecule and enzymatic contributions to total antioxidant capacity across development, as well as in adult tissues. Finally, we determine the effects of anoxia/reperfusion on SOD activity, and discuss our findings in a comparative context.

Materials and methods

Chemicals

All chemicals were purchased from Sigma-Aldrich (St. Louis, MO, USA), unless otherwise noted.

*Husbandry of adult *A. limnaeus* and the collection of embryos*

Adult *A. limnaeus* were reared in the Aquatic Vertebrate Facility at Portland State University as previously described (Podrabsky, 1999) and according to protocols approved by the PSU Institutional Animal Care and Use Committee (PSU protocol #33). Spawning pairs were housed in 9.5 l glass aquaria with 21 tanks connected to a shared sump and recirculating filtration system. Systems were filled with charcoal filtered and UV sterilized City of Portland water supplemented with 0.115% Coralife sea salt (Central Aquatics, Franklin, WI, USA). Water changes (10% of total system volume) were performed twice daily. Temperature was regulated at $27 \pm 1^\circ\text{C}$ and photoperiod was maintained at 14L:10D. Adult fish were fed Hikari frozen bloodworms (Chironomid larvae, Kyorin Co, Ltd., Japan) twice daily and chopped red wiggler earthworms twice weekly, on the day before spawning.

Embryos were collected twice a week (Podrabsky, 1999). Embryos were maintained in 100 x 15 mm plastic culture dishes containing 50-100 embryos/dish depending upon age. Embryo medium (10 mmol l⁻¹ NaCl, 0.1424 mmol l⁻¹ KCl, 2.15 mmol l⁻¹ MgCl₂, 0.0013 mmol l⁻¹ MgSO₄, 0.92 mmol l⁻¹ CaCl₂, in reagent grade water) was changed daily. To reduce fungal infections, 0.0001% methylene blue was added for the first 4 d post-fertilization (dpf) and at 4 dpf embryos were treated with two washes of 0.03% sodium hypochlorite (5 min each with a 5 min rest between) as described previously (Podrabsky, 1999). Subsequently, embryos were rinsed for 10 min in 0.005% sodium thiosulfate to ensure neutralization of the hypochlorite. Embryos were then transferred into embryo medium containing 10 mg l⁻¹ gentamicin sulfate (Amresco, Solon, OH, USA). Embryos were incubated at 25°C in incubators (Sheldon Laboratories, Cornelius, OR, USA) under dark conditions to prevent the breaking or bypassing of DII (Podrabsky et al., 2010; Podrabsky and Hand, 1999; Romney et al., 2018).

Developmental staging and sampling of embryos

Embryos were staged by age (dpf) for early development through diapause II. Embryos that enter DII at 22-24 dpf are characterized by two conditions: a heart rate of less than 10

beats/min and the presence of 38-42 somite pairs along the central axis (Podrabsky et al., 2017; Podrabsky and Hand, 1999). DII was broken by exposure to continuous light at 30°C for 48 h (Meller et al., 2012). Post-diapause II (PDII) embryos were staged and sorted daily according to Wourms' stage (WS) definitions updated by Podrabsky et al. (Podrabsky et al., 2017). Age of PDII embryos is provided in days post-diapause II (dpd). As illustrated by Podrabsky and Hand (Podrabsky and Hand, 1999), embryonic metabolism peaks at 18-20 dpd and spontaneous hatching is typically seen during this time period. Embryos that fail to hatch after 24 dpd are considered to be entering DIII (Podrabsky and Hand, 1999). Typically, embryos from a single spawning date were used to represent a single replicate. However, at times, multiple spawning events were pooled together. In all experiments, three or more spawning events or pooled samples are represented (n=3-4).

Tolerance of hydrogen peroxide

Tolerance of exposure to exogenous hydrogen peroxide (H₂O₂) was assessed by incubating whole embryos in solutions of H₂O₂ diluted in embryo medium. Embryos were treated at 5 developmental stages across embryonic development: WS 24/25 (8 dpf), WS 32/D2 (32-50 dpf), WS 36 (4 dpd), WS 40 (12 dpd), and WS 43 (24 dpd). For each stage, three replicates of 20 embryos were placed in plastic culture dishes containing solutions of H₂O₂ ranging from 0 – 5%. Media was changed daily. Survival was monitored at 4, 12, 19, 24, 48 and 72 h post-exposure. Dead embryos were identified by their notably opaque white coloration and/or rupturing of the embryo and were removed at each time point. For WS 43 embryos, those that hatched were also removed, although all hatched embryos died quickly in even the lowest concentrations of H₂O₂.

Exposure of embryos to anoxia

Embryos were exposed to anoxia in a Bactron III anaerobic chamber (Sheldon Manufacturing, Cornelius, OR, USA) that uses a mix of 5% hydrogen, 5% carbon dioxide, and 90% nitrogen gas. The chamber maintains a slight positive pressure of this gas mixture and contains a palladium catalyst that converts oxygen to water in the presence of hydrogen gas. Embryos were collected and incubated as describe above. Aerobic medium was poured out of the culture places and the embryos placed into the chamber through a pass box that preserves the anoxic environment inside the chamber. Once inside the chamber the embryos were immediately placed into anoxic medium. Embryos were exposed to anoxia for 48 h and then returned to aerobic conditions to recover for 24 h.

Oxygen radical absorbance capacity (ORAC) assay

Preparation of sample homogenates. Groups of 30 embryos were blotted dry and weighed immediately prior to homogenization. Various tissues from adult females were also sampled for comparative purposes (n=3). Samples were homogenized in tapered ground-glass tissue grinders on ice in a 1:9 ratio (m/v) of embryos/tissue to ice-cold 75 mmol l⁻¹ sodium phosphate buffer (pH 7.4 at 25°C). The crude homogenate was collected into a 1.5 ml microcentrifuge tube and briefly sonicated at an amplitude of 20% for 10 s (Branson Digital Sonifier, S-450D). Half the homogenate was then mixed 1:1 with 20% meta-phosphoric acid (prepared fresh daily) and incubated on ice for 5 min to precipitate proteins and other large. Acid extracts, which contain the small molecule antioxidants, were subjected to centrifugation at 16,000 x g for 20 min at 4°C to pellet insoluble materials. The acid-soluble supernatant was then carefully transferred into a 1.5 ml microcentrifuge tube on ice. All samples were tested at a final dilution of 400X. For the acid soluble fraction the final concentration of meta-phosphoric acid in the assay was 0.25%.

ORAC assay. ORAC activity in both whole embryo extracts as well as the protein-free fraction of embryo extracts was determined as described previously (Ninfali and Aluigi, 1998). The assay measures the protection of the decay of fluorescein as a result of oxidative damage by peroxy-radicals generated by the addition of AAPH [2,2'-Azobis(2-amidinopropane) dihydrochloride] (Zulueta et al., 2009). Trolox, a water soluble analog of vitamin E, was used as a standard antioxidant to generate a standard curve and thus the ORAC activity of a sample is expressed in trolox equivalents. Solutions of fluorescein (48 nmol l^{-1}) and AAPH (240 mmol l^{-1}) were prepared fresh daily. A 200 mmol l^{-1} stock of trolox was prepared in 75 mmol l^{-1} phosphate buffer (pH 7.4 at 25°C) and frozen in aliquots at -20°C . A trolox standard curve was prepared by serial dilution of a $100 \text{ }\mu\text{mol l}^{-1}$ solution in phosphate buffer to yield concentrations of 100, 50, 25, 12.5, 6.25, 3.125, and $0 \text{ }\mu\text{mol l}^{-1}$.

Embryo homogenate ORAC activity was tested in a total volume of $200 \text{ }\mu\text{l}$ with a final concentration of 36 nmol l^{-1} fluorescein and 30 mmol l^{-1} AAPH in 75 mmol l^{-1} sodium phosphate buffer (pH 7.4). The sample/standards ($25 \text{ }\mu\text{l}$) and fluorescein ($150 \text{ }\mu\text{l}$) were added to wells of a flat bottom black polystyrol 96-well plate and incubated at 37°C for 20 min, followed by the addition of $25 \text{ }\mu\text{l}$ of 240 mmol l^{-1} AAPH to start the assay. Fluorescein fluorescence was measured at 37°C with a plate reader in top read mode (Tecan Infinite M200 Pro, Männedorf, Switzerland). Excitation and emission wavelengths were set to 485/535 nm with band widths of 9/20 nm, respectively. Readings were obtained every 150 s for 30 min with 10 s of shaking (linear, 1 mm amplitude) prior to each measurement. Fluorescence gain was manually set to 100 based on preliminary experiments. Samples were excited with 30 flashes of light and emission of light was integrated over $150 \text{ }\mu\text{s}$ following excitation. The optimal z-position for each plate/assay was automatically calculated from a standard well at the beginning of each assay. ORAC activity was determined by plotting the decrease in fluorescence over time and determining the area under the curve (AUC) for each standard and sample (GraphPad Prism, version 5). A standard curve of AUC versus trolox concentration was used to interpolate the

ORAC activity in each sample in $\mu\text{mol l}^{-1}$ trolox equivalents. These values were then used to calculate ORAC activity in mmol kg^{-1} for embryos and adult tissues.

Total glutathione content

Total glutathione was quantified using an Assay Designs/Stressgen kit according to the manufacturer's instructions (Enzo Life Sciences, Inc., Farmingdale, NY, USA). Groups of 30 embryos from 3-4 spawning events were blotted dry, weighed, and immediately homogenized in 19 volumes (m/v) of 5% meta-phosphoric acid. Acid homogenates were subjected to centrifugation at $16,000 \times g$ for 10 min at 4°C to pellet insoluble materials. Acid supernatants ($50 \mu\text{l}$) were added to $150 \mu\text{l}$ of freshly prepared reaction mix and absorbance at 405 nm (A_{405}) was measured for 10 min at room temperature using a plate reader. All samples and standards were assayed in triplicate. A standard curve for total glutathione was generated by calculating the slope of increase in A_{405} over time and plotting the slope as a function of total glutathione concentration in the well. Total glutathione in the samples was then determined by interpolation of slopes. Oxidized glutathione was determined as above except that the samples and standards were first treated with 4-vinylpyridine. Reduced glutathione was calculated by subtracting the oxidized levels of glutathione from the total.

Catalase activity

Catalase activity was measured indirectly using a modified amplex red assay (Keilin and Hartree, 1934; Mueller et al., 1997; Zhou et al., 1997). Groups of 30 embryos were weighed and homogenized at a dilution of 20X (1:19 m/v) with ice-cold 75 mmol l^{-1} sodium phosphate buffer (pH 7.4 at 25°C) in tapered ground-glass tissue grinders on ice. Crude homogenates were collected in 1.5 ml microcentrifuge tubes, vortexed, and sonicated for 10 s as described above. Homogenates were then subjected to centrifugation at $10,000 \times g$ for 15 min at 4°C to pellet

large pieces of insoluble debris. Supernatants were carefully transferred into 1.5 ml microcentrifuge tubes and placed on ice prior to determination of catalase activity. Aliquots of each homogenate were incubated in a final concentration of 0.75 mmol l⁻¹ sodium azide for 5 min prior to initiation of the assay to inhibit catalase activity. Embryo homogenates (with and without sodium azide) were added to ice-cold working reagent (prepared fresh daily) consisting of 75 mmol l⁻¹ sodium phosphate buffer (pH 7.4 at 25°C), 0.04 U ml⁻¹ horseradish peroxidase, and 10 mmol l⁻¹ amplex red in flat-bottom black polystyrol 96 well plates. Total volume in each well was 100 µl. After a 10 min incubation at 25°C, 10 µl of 0.1 mmol l⁻¹ H₂O₂ was added to each well to start the reaction. The reaction was incubated at 25°C for 10 min, before termination by the addition of sodium azide. Fluorescence was measured at excitation/emission wavelengths of 540/590 nm using a plate reader (Tecan) in top read mode every 90 s for 45 min, with 10 s of linear shaking (1 mm amplitude) prior to each reading, and temperature maintained at 25°C. Gain was manually set to 61 (based on preliminary experiments) and 50 flashes were used for each reading with an integration time of 20 µs. The z-position was automatically calculated from well A1. The amount of residual H₂O₂ in each homogenate was compared to H₂O₂ standards ranging from 0 – 10 µmol l⁻¹. Catalase-specific activity was determined by subtracting the azide-inhibited rate of H₂O₂ conversion from the total rate for each sample.

Superoxide dismutase activity

Superoxide dismutase (SOD) activity was measured using a modified spectrophotometric method utilizing WST-1 (4-[3-(4-iodophenyl)-2-(4-nitrophenyl)-2H-5-tetrazolio]-1,3-benzene disulfonate, from Dojindo Lab) (Peskin and Winterbourn, 2000)(Ishiyama et al., 1993)(Ukeda et al., 1999). Groups of 30 embryos were homogenized (1:19 m/v) in ice-cold 50 mmol l⁻¹ sodium phosphate buffer (pH 8 at 25°C). Crude homogenates were transferred to 1.5 ml microcentrifuge tubes, vortexed, sonicated, and subjected to centrifugation as described above for the catalase assay. Cleared supernatants (20 µl) were

added to 200 μl assay cocktail consisting of 50 mmol l^{-1} sodium phosphate (pH 8 at 25°C) containing 0.1 mmol l^{-1} pentetic acid, 0.4 mmol l^{-1} xanthine, and 1 mmol l^{-1} WST-1 in wells of a polystyrol transparent and flat bottom 96 well plate. The assay was initiated by addition of xanthine oxidase to a final concentration of 4 mU ml^{-1} . A standard curve (0-10 $\mu\text{g ml}^{-1}$) of purified SOD was prepared and run in parallel to the samples. Absorbance at 438 nm (25 flashes per measurement) was monitored for 20 min at 25°C using a plate reader. Prior to each measurement the plate was mixed by linear shaking for 10 sec with a 1 mm amplitude.

Glutathione Peroxidase Activity

Glutathione peroxidase (GPx) activity was measured spectrophotometrically by coupling the oxidation of glutathione and NADPH using glutathione reductase, thus recycling GSSG to its reduced state (Paglia and Valentine, 1967) as modified by Gallo and Martino (Gallo and Martino, 2009). Embryos (n = 10 per sample) were collected and homogenized (1:9, w/v) as described above (see catalase assay) in ice-cold 50 mmol l^{-1} sodium phosphate buffer (pH 8.0 at 25°C). Cleared supernatants were used for all assays. Sample homogenates or standards (10 μl) were added to 180 μl assay buffer consisting of 50 mmol l^{-1} sodium phosphate buffer (pH 8.0), 5 mmol l^{-1} EDTA, 1.5 mmol l^{-1} sodium azide, 5.0 mmol l^{-1} GSH, and 4.5 U ml^{-1} glutathione reductase. Background degradation of NADPH was recorded by measuring absorbance at 430 nm (25 flashes per reading) every 60 seconds for 5 minutes, preceded by 10 seconds of linear shaking (amplitude 1 mm). The reaction was initiated by the addition of 10 μl of 2.4 mmol l^{-1} cumene hydrogen peroxide (0.12 mmol l^{-1} final concentration) to each well followed by an additional 5 min of data collection as described above.

Quantification of total embryonic DNA

For normalizing enzymatic activities, total DNA in embryo homogenates was quantified using the Quant-iT Broad-Range DNA Assay Kit (Life Technologies, Eugene, OR, USA) using the manufacturer's instructions. Fluorescence was measured using a Tecan plate reader with excitation/emission wavelengths and bandwidths set at 485/535 nm and 9/20 nm, respectively. The gain was set manually at 95, with 30 flashes per measurement and a 20 μ s integration time. The Z-position was calculated automatically from well A1. All readings were collected at 25°C. DNA concentration in embryo homogenates was determined by interpolation against a DNA standard curve provided in the kit.

Monitoring of post-diapause II development in H₂O₂ exposed DII embryos

Three replicates of DII embryos (n=10 per replicate) were exposed to 5% H₂O₂ in embryo media for 0, 1, or 3 h at room temperature in plastic culture dishes subjected to gentle rotation. Following treatment, embryos were rinsed several times in fresh embryo media and incubated at 25°C in darkness. Embryos were examined at 11 days post-H₂O₂ exposure to determine if they had morphological characteristics of PDII development, such as red blood cells, melanocytes, and eye pigmentation (Podrabsky et al., 2017).

RNAseq data and identification of antioxidant enzyme orthologs

Antioxidant enzyme orthologs were identified from the *Austrofundulus limnaeus* genome annotation version 100 in the NCBI GenBank database (Wagner et al., 2018). RNAseq data were obtained from data sets deposited in GenBank (Bioproject PRJNA272154). Data for early

embryos developing at 20°C are from Romney et al. (2018). Data for diapause II and 4 dpd embryos at 25°C are from Wagner et al. (2018). Data for embryos at 12 and 20 dpd at 25°C have not been previously published.

Statistics

Survival curves were generated using Prism version 7.0 software (GraphPad Software, La Jolla, CA, USA). Lethal time to 50% mortality was calculated using Probit regression analysis (SPSS, IBM Analytics, Armonk, NY, USA) on the data expressed as a proportion. To compare group means, one-way Analysis of Variance (ANOVA) followed by Tukey's Multiple Comparison Test (Tukey's MCT) was applied to the enzyme assays and total and percent reduced glutathione concentration using GraphPad Prism (v7.0, La Jolla, CA, USA). To compare group means in the PDII development of H₂O₂ exposed DII embryos, one-way ANOVA statistics were applied to the arcsine transformation of the square root of the proportions, and were followed by Tukey's MCT (Zar, 1996). Correlation analysis comparing SOD and catalase activity was performed in Prism 7.0 using default settings. For correlations, a P value of less than 0.05 indicates that the slope is significantly non-zero. Prior to correlation analysis, the Prism 7.0 ROUT method was performed on the data to find statistical outliers with Q = 5%. If there are outliers in a dataset, the ROUT Q value is equal to the maximum false discovery rate.

Results

Tolerance of hydrogen peroxide

Tolerance of H₂O₂ increased during early development and peaked during diapause II (Figs. 1,2). During DII only the 3 and 5% treatments caused any mortality during the 72 h exposures. Tolerance was then lost during PDII development with DIII embryos exhibiting the

lowest tolerance of any stage. When the survival data were used to estimate a lethal time to 50% mortality (LT_{50}), tolerance of H_2O_2 peaked during DII, with mean (\pm sem) LT_{50} values of $15.9 \pm .85$ and 33.5 ± 1.3 h for 5% and 3% H_2O_2 , respectively (Fig. 2). This tolerance of H_2O_2 was retained in embryos at 4 dpd and then declined to 4.5 ± 0.8 and 5.9 ± 1.2 h (5% and 3%, respectively) when embryos complete embryonic development and enter DIII at WS 43.

H₂O₂ treatment did not cause embryos to exit diapause II

Following sublethal treatment of 5% H_2O_2 for 1 or 3 h, embryos did not exit DII at a higher rate than unexposed controls (Fig. S1, one-way ANOVA, $P = 0.166$).

Whole embryo oxygen radical absorbance capacity

Whole-embryo ORAC remained relatively constant through development, ranging from 30-45 mmol kg⁻¹ embryo (Fig. 3A, one-way ANOVA, $p = 0.1$). In early development through DII the acid supernatant (small molecule) fraction remained relatively constant and represented $74.6 \pm 1.8\%$ of the capacity across all early developmental stages (Fig. 3B). During PDII development a dramatic shift occurred in the proportion of the whole embryo ORAC that is invested in the small molecules (Fig. 3B, one-way ANOVA, $p < 0.0001$). The majority of the ORAC shifted from $61 \pm 0.3\%$ invested in the small molecule fraction during the first 12 days of PDII development to being dominated by the macromolecule fraction ($93.4 \pm 6.2\%$) in WS 43 embryos at 22 dpd (Fig. 3B). When compared to tissues from adults, whole-embryo ORAC was most similar to that observed in ovary tissue both in magnitude and proportion of the capacity that is due to small molecules. Additionally, the ovary tissue also had the highest acid supernatant ORAC activity when compared to other adult tissues (one-way ANOVA with Tukey's MCT, $p < 0.05$, Fig. 3C).

Total glutathione levels, but not percent reduced, changed across embryonic development

Total GSH levels remained low and relatively constant (35-23 $\mu\text{mol kg}^{-1}$) during early development through DII (Fig. 4A). After embryos broke DII, total GSH levels increased significantly until reaching 180 $\mu\text{mol kg}^{-1}$ at 12 dpd and remained constant until 25 dpd (one-way ANOVA with Tukey's MCT, $P < 0.001$). Total GSH includes both oxidized and reduced forms, and the glutathione pool remained near 100% reduced for all of development, with a slightly lower but not statistically-significant reduction at 8 dpf (Fig. 4B, one-way ANOVA, $p=0.084$).

*Antioxidant enzyme activity was dynamic across normal *A. limnaeus* development*

When expressed per unit DNA, enzyme activities of the three antioxidant enzymes were generally higher during early development through DII, reaching their lowest activities during PDII development (Fig. 5). Catalase activity in early embryos through DII remained high, followed by a significant decrease during PDII development when compared to DII embryos (one-way ANOVA with Tukey's MCT, $p < 0.05$). In contrast, SOD and GPx activities expressed per unit DNA steadily declined throughout development and reached their lowest levels at the end of embryonic development (one-way ANOVA with Tukey's MCT, $p < 0.05$). The overall patterns of SOD, catalase, and GPx activity per unit of DNA matched transcript expression patterns for the enzymes, with generally higher levels of transcripts early in development and lower levels in PDII stages (Fig. 6A). Transcripts for several peroxiredoxin paralogs were observed to be expressed during embryonic development, with expression of peroxiredoxin 5 being maintained substantially throughout pre-diapause II development (Fig. 6B). In addition, several enzymes involved in maintaining GSH synthesis and oxidative state, protein components of the glutaredoxin and thioredoxin systems, as well as other antioxidant-related proteins were identified to be expressed during development, but at comparatively low levels (Fig. 6C-E).

SOD and catalase activity correlated strongly across development

We observed significant correlation of SOD and catalase activity when enzyme activity was expressed per g embryo (Fig. 7A, $r = -0.7$, $p = 0.0075$) or per μg DNA (Fig. 7B, $r = 0.86$, $p = 0.003$). These two correlations were inverted, with activity expressed per g embryo (Fig. S2) exhibiting a strong negative correlation and activity expressed per μg DNA exhibiting a strong positive correlation. One statistical outlier was identified using the Prism ROUT method for the 0 dpf embryos when activity was expressed per unit DNA and this data point was omitted from the correlation analysis (Fig. 7B, open circle).

SOD activity is not responsive to anoxia or recovery from anoxia

When embryos at 4 or 16 dpd were exposed to anoxia, SOD activity was stable for 48 h and did not increase significantly after 24 h of aerobic recovery (Fig. S3, one-way ANOVA, $p = 0.8$ for 4 dpd embryos, and $p = 0.3$ for 16 dpd embryos).

Discussion

Of all the developmental stages, DII embryos (WS 32) are known to be the most stress-tolerant to anoxia, ultraviolet-C radiation exposure, salinity, and desiccation, and it is during this stage that annual killifishes are thought to survive the dry season (Machado and Podrabsky, 2007; Podrabsky et al., 2016; Podrabsky et al., 2001; Podrabsky et al., 2007; Wagner and Podrabsky, 2015; Wourms, 1972c). This extreme stress tolerance of DII embryos has also been shown to extend until 4 dpd (WS 36), and in line with these previous observations, *A. limnaeus* DII and 4 dpd have the highest tolerance to H_2O_2 . We were unable to observe significant death in DII or 4 dpd embryos at 1% H_2O_2 exposure after 72 hours, and it is possible that these embryos

would be able to tolerate this concentration for extended lengths of time similar to anoxia (Podrabsky et al., 2007). In aquaculture, H₂O₂ treatment has been used to sterilize fish eggs with non-toxic doses appearing to be largely species dependent. Exposure ranges from 0.01 – 0.025% and exposure times on the order of minutes are most commonly used (Chambel et al., 2014; De Swaef et al., 2016; Matthews et al., 2012). Although LD₅₀ values are generally absent for other fish embryo species exposed to H₂O₂, embryos of the channel catfish *Ictalurus punctatus* have reduced hatching success after a single 15 min exposure to 0.05% H₂O₂, while early embryos of the cutthroat trout *Oncorhynchus clarkia* had increased mortality after only a 2 min exposure to 1.5% H₂O₂ (Small and Wolters, 2003; Wagner et al., 2012). Even at developmental stages that are overall less stress-tolerant, *A. limnaeus* embryos were able to tolerate 1% H₂O₂ for nearly a day before reaching LT₅₀. Thus, the data presented provide evidence for substantial tolerance of H₂O₂ in embryos of *A. limnaeus* during normal development, and extreme tolerance during DII. We did not follow H₂O₂-exposed embryos during post-hatching development, and it would be interesting to observe any long-term effects of embryonic H₂O₂ exposure on physiology or fecundity of later life history stages.

Surprisingly, H₂O₂ exposure had no effect on termination of diapause. Our finding contrasts with previous work in encysted embryos of the brine shrimp *Artemia*, which showed that *Artemia* diapause can be efficiently terminated using H₂O₂ exposure (Robbins et al., 2010). It is possible that in *Artemia* the ROS generated by H₂O₂ exposure or the H₂O₂ molecule itself activates signaling cascades, which promote resumption of development. Although *A. limnaeus* and *Artemia* share very similar life histories and responses to environmental stress, our results agree with previous work that suggest unique signaling mechanisms in the two lineages which cue for entrance and exit from diapause (Podrabsky and Hand, 2015). *A. limnaeus* embryos have been previously shown to bypass diapause following increased temperature and light exposure, and this mechanism is mediated by the vitamin D signaling pathway (Podrabsky, 1999; Podrabsky et al., 2010; Romney et al., 2018). The role of vitamin D signaling in initiating exit from diapause in *A. limnaeus* diapause remains unclear. We hypothesize that vertebrate anoxia

tolerance may require embryos to have rapid ROS quenching, and therefore H_2O_2 is rapidly converted to oxygen and water before it can act as a signal for diapause exit. We cannot exclude the possibility that external H_2O_2 may be prevented from reaching deep embryonic tissues in the first place, but our results suggest there is an ROS-independent mechanism for diapause exit (e.g. vitamin D signaling) that may distinguish *A. limnaeus* from *Artemia*.

The reason for the extreme tolerance to H_2O_2 observed in *A. limnaeus* embryos is unclear, although it may be related to the excessive tolerance often observed in organisms with the ability to enter into metabolic dormancy (Jonsson, 2003). Surprisingly, antioxidant enzyme capacity per unit DNA and mRNA transcript levels are highest in early embryos and steadily decline during development and entrance into DII. This pattern is indicative of maternal provisioning and suggests that the highest level of per-cell antioxidant enzyme protection occurs early in development. There is a clear break in the expression pattern between pre-diapause II and post-diapause II development, suggesting maternal proteins and transcripts may dominate antioxidant capacity in early development through DII, while embryonic expression becomes much more important during late development. Notably, the loss of total antioxidant enzyme capacity in late embryos along with the decline in small molecule antioxidant capacity correlates with their loss of long-term anoxia tolerance. Also coinciding with the resumption of development, we observed a significant increase in embryonic total reduced GSH. While PDII embryos have the highest levels of total reduced GSH, previous work has suggested that GPx may not be a primary ROS defense mechanism in anoxia-sensitive tissues, which may explain in part why later embryonic stages have the highest levels of GSH but anoxia tolerance is low relative to earlier stages (Marchena et al., 1974). With enzymatic activity per unit DNA (a proxy for per cell) stable or decreasing during early development, and overall antioxidant capacity remaining relatively stable, it appears that other factors must be at work to explain the peak H_2O_2 tolerance observed in DII embryos. One possible explanation is a reduced permeability of the embryo's enveloping cell layer to small molecules which would slow entry of the H_2O_2 into the embryo. Like water, H_2O_2 is a polar molecule and cannot quickly travel across

biological membranes without the assistance of integral membrane channels such as aquaporins (Bienert et al., 2006). Decreased expression of these integral membrane proteins on the surface of the enveloping cell layer could help slow the entrance of H₂O₂ from reaching sensitive embryonic tissues. This theory is further supported by a remarkable decrease in the permeability to water and ions during early development in embryos of *A. limnaeus* (Machado and Podrabsky, 2007). It is critical to note that the major permeability barrier in these embryos is not the egg envelope, but rather appears to be the enveloping cell layer (ECL), the outer most syncytial cell layer of the embryo (Machado and Podrabsky, 2007). Interestingly, ECL acts as an extraembryonic membrane in annual killifishes and is shed at hatching. Thus, this cell layer may be specialized to withstand severe oxidative stress, and perhaps the high levels of mRNA transcripts for the membrane-associated form of GPx and the extracellular form of SOD (see discussion below) are working in concert with the low permeability of the ECL to protect the deeper embryonic tissues from oxidative damage. However, direct evidence of a role for reduced transmembrane transport of H₂O₂ and the cellular location of antioxidant enzymes remains to be determined.

Extreme tolerance to H₂O₂ exposure may yield insight into strategies that permit long-term anoxia tolerance, and perhaps more importantly, resumption of normal development following reoxygenation in *A. limnaeus*. Following ischemia/reperfusion, oxygen-sensitive mammalian cells are thought to experience mitochondrial biogenesis driven by an increase in ROS (Lee and Wei, 2005; Li et al., 2012; Yin et al., 2008). However, it has been previously reported that *A. limnaeus* embryos do not experience significant mitochondrial biogenesis following conditions similar to ischemia/reperfusion, and this was hypothesized to be due to rapid ROS quenching (Wagner et al., 2016). Supporting this hypothesis is our observation that embryos with the highest overall anoxia tolerance also appear to obtain most of their antioxidant capacity from small molecules. Using small molecules to rapidly quench ROS following anoxia/reoxygenation would in principle prevent macromolecule oxidative damage and may be a similar strategy to that of other anoxia-tolerant vertebrates, such as the

freshwater turtle (Lutz and Milton, 2004; Milton et al., 2007; Willmore and Storey, 1997). Small molecule antioxidants include molecules such as ascorbic acid (Vitamin C), which have been implicated in freshwater turtle brain anoxia tolerance, and may be one of the primary antioxidants (Rice et al., 1995). Importantly, some small molecule antioxidants (e.g. ascorbic acid) must be obtained by diet in fishes, and thus levels of these compounds may be limited to maternal packaging. This would explain why we observe small molecule antioxidant capacity decreasing substantially over embryonic development. Notably, we observed the highest ORAC activity from small molecules in ovary tissue compared to other adult tissues tested, supporting a potential route for maternal packaging of these components. Anoxia tolerance is therefore achieved through a combination of low metabolic demand, differential gene expression, and the presence of small molecule antioxidants (Podrabsky and Hand, 1999; Wagner et al., 2018). This strategy may also contribute to their excessive tolerance to abiotic oxidant exposure, such as the H_2O_2 used in this study; however, the identity of the small molecules that protect early embryos of *A. limnaeus* from oxidative damage are currently unknown.

The *A. limnaeus* whole-embryo ORAC assays revealed a clear switch from small molecule antioxidant capacity to macromolecule antioxidant capacity towards the end of embryonic development. If enzymatic activity is expressed per g embryo, the overall majority of enzymatic antioxidant activity towards the end of development may be due to catalase and GPx activity, but not SOD. A similar trend was found in turbot *Scophthalmus maximus* L. where embryos had higher catalase and total GPx activity after hatching, but SOD decreased, when normalized to total protein (Peters and Livingstone, 1996). While expression of enzyme activity per g embryo or per g protein may be appropriate for individual tissues, fish embryos are generally closed systems with respect to metabolism because they obtain their nutrients from maternally provisioned yolk. In *A. limnaeus*, whole embryo protein content decreases by 22% during early development as embryos enter into DII, while cell number and DNA content clearly increase (Podrabsky and Hand, 1999). Normalization of enzymatic activity to total protein content of embryos that includes yolk may provide a misleading estimation of activity that is relevant to

developing embryonic tissues. Therefore, in addition to normalization of enzymatic activity to total embryonic wet mass, we also showed enzymatic activity normalized to total embryonic DNA, which increases as embryonic cells divide (Podrabsky and Hand, 1999). Paradoxically, we observed a negative correlation between catalase and SOD activity when measured as a function of embryo mass. The expected positive relationship between the activity of these two enzymes that must work in concert to detoxify superoxide anions, the most common form of ROS in mitochondria, suggests that interpretations of these data normalized to DNA content are most likely to reflect the *in vivo* capacity of these enzymes at the cellular level (Jenkins et al., 1984). This conclusion is also supported by patterns of mRNA expression across development that are similar to enzyme activity data expressed per unit DNA. However, how tightly the activity of catalase and SOD are coupled at the embryonic-cell level, remains to be determined.

Cells contain a variety of antioxidant enzyme systems to protect against oxidative damage in various organ systems, or within specific subcellular compartments. It is possible that the subset of antioxidant enzyme systems expressed during development of *A. limnaeus* may contribute to their unique capabilities to survive oxidative damage and long-term anoxia. For example, there are many isoforms of GPx and SOD encoded in vertebrate genomes, and *A. limnaeus* is no exception. All three forms of SOD are expressed during early development, with the cytoplasmic (soluble) form expressed at the highest level in terms of transcript abundance. In fact, the cytoplasmic form is almost always expressed at a higher level than the mitochondrial form for the duration of development. This is a curious pattern, given that superoxide anions are typically produced in the mitochondrion, but may be consistent with the low rates of oxidative metabolism and restricted mitochondrial activity in *A. limnaeus* embryos. Also of interest is the sustained expression of the extracellular form of SOD throughout development which may help to protect the embryo from external ROS production, especially if it is exported into the perivitelline space. We make this suggestion based on the fact that its highest expression level is observed early in development, long before the circulatory or lymphatic systems are formed and functioning. Interestingly, we observed no change of SOD activity in 4

dpd and 12 dpd embryos exposed to anoxia/reoxygenation. This lack of change agrees with previous transcriptome work suggesting that anoxia-tolerant 4 dpd embryos do not differentially express SOD variants following anoxia exposure, and suggests that antioxidant capacity prior to anoxia may be more critical than induction of enzyme systems in response to anoxia (Podrabsky et al., 2007; Wagner et al., 2018). Of the many forms of GPx encoded in the *A. limnaeus* genome, GPx4 is by far the most abundantly expressed transcript in these embryos. Interestingly, GPx4 is known to associate with membranes and is able to detoxify a variety of peroxides, including hydroperoxides of complex lipids and cholesterol derivatives within membranes (Brigelius-Flohé and Maiorino, 2013). This activity may help to protect membranes from oxidative damage during transitions into and out of hypoxia/anoxia or as a result of environmental sources. Lastly, peroxiredoxin 5 is highly expressed in early embryos. This peroxidase has been shown to protect against excitotoxic brain lesions in newborn mice (Plaisant et al., 2003), and to prevent apoptosis and extend lifespan in *Drosophila* through reduction of oxidative stress (Radyuk et al., 2009). Thus, the role of this particular protein in the antioxidant arsenal of *A. limnaeus* deserves additional study.

Conclusions

Embryos of *A. limnaeus* have an impressive tolerance of oxidative stress and can survive for days in 1% H₂O₂. Measures of total antioxidant capacity suggest that embryos with high tolerance of anoxia also have a high proportion of their antioxidant capacity invested in small molecules, and the loss of these small molecules is correlated with a substantial decrease in tolerance of anoxia. At the per-cell level, enzymatic antioxidant systems in *A. limnaeus* are highest in early development and decrease substantially during PDII development when extreme anoxia tolerance is lost. Thus, at the cellular level early embryos have the highest antioxidant capacity consistent with their higher tolerance of anoxia. Early embryos, especially those in DII, have extremely low permeability to water and thus it is also likely that specialized

embryonic membranes contribute to extreme tolerance of H₂O₂. Embryos of *A. limnaeus* present a unique model for studies of antioxidant activity due to the interplay between maternal packaging and ontogenetic changes in embryonic structure and gene expression of antioxidant systems. Future alteration of maternal diet and gene expression may allow for experimental manipulations in this system that can help to define the role of antioxidant capacity in supporting long-term tolerance of anoxia.

Acknowledgements

The authors would like to thank Drs. Amie Romney and Claire Riggs for their work in the preparation of the RNAseq data included in this manuscript.

Competing Interests

No competing interests declared.

Funding

This work was supported by the National Science Foundation [IOS- 1354549 to J.E.P.].

References

- Bienert, G. P., Schjoerring, J. K. and Jahn, T. P.** (2006). Membrane transport of hydrogen peroxide. *Biochim Biophys Acta Biomembr* **1758**, 994-1003.
- Brigelius-Flohé, R. and Maiorino, M.** (2013). Glutathione peroxidases. *Biochim Biophys Acta Gen Subj* **1830**, 3289-3303.
- Cao, W., Carney, J., Duchon, A., Floyd, R. and Chevion, M.** (1988). Oxygen free radical involvement in ischemia and reperfusion injury to brain. *Neurosci Lett* **88**, 233-238.
- Chambel, J., Costa, R., Gomes, M., Mendes, S., Baptista, T. and Pedrosa, R.** (2014). Hydrogen peroxide, iodine solution and methylene solution highly enhance the hatching rate of freshwater ornamental fish species. *Aquacult Int* **22**, 1743-1751.
- Chennault, T. and Podrabsky, J. E.** (2010). Aerobic and anaerobic capacities differ in embryos of the annual killifish *Austrofundulus limnaeus* that develop on alternate developmental trajectories. *J Exp Zool A* **313A**, 587-596.
- De Swaef, E., Van den Broeck, W., Dierckens, K. and Decostere, A.** (2016). Disinfection of teleost eggs: a review. *Rev Aquac* **8**, 321-341.
- Drouin, G., Godin, J.-R. and Pagé, B.** (2011). The genetics of vitamin C loss in vertebrates. *Curr Genomics* **12**, 371-378.
- Duerr, J. M. and Podrabsky, J. E.** (2010). Mitochondrial physiology of diapausing and developing embryos of the annual killifish *Austrofundulus limnaeus*: implications for extreme anoxia tolerance. *J Comp Physiol B* **180**, 991-1003.
- Gallo, G. and Martino, G.** (2009). Red blood cell glutathione peroxidase activity in female nulligravid and pregnant rats. *Reprod Biol Endocrinol* **7**, 7.
- Gerhard, G. S., Kauffman, E. J. and Grundy, M. A.** (2000). Molecular cloning and sequence analysis of the *Danio rerio* catalase gene. *Comp Biochem Physiol B Biochem Mol Biol* **127**, 447-457.
- Hrbek, T., Taphorn, D. C. and Thomerson, J. E.** (2005). Molecular phylogeny of *Austrofundulus* Myers (Cyprinodontiformes: Rivulidae), with revision of the genus and the description of four new species. *Zootaxa* **825**, 1-39.
- Ishiyama, M., Shiga, M., Sasamoto, K., Mizoguchi, M. and He, P.-g.** (1993). A new sulfonated tetrazolium salt that produces a highly water-soluble formazan dye. *Chem Pharm Bull* **41**, 1118-1122.
- Jenkins, R., Friedland, R. and Howald, H.** (1984). The relationship of oxygen uptake to superoxide dismutase and catalase activity in human skeletal muscle. *Int J Sports Med* **5**, 11-14.
- Jonsson, I. K.** (2003). Causes and Consequences of Excess Resistance in Cryptobiotic Metazoans. *Physiol Biochem Zool* **76**, 429-435.
- Keilin, D. and Hartree, E.** (1934). Inhibitors of catalase reaction. *Nature* **134**, 933.
- Kirino, T.** (1982). Delayed neuronal death in the gerbil hippocampus following ischemia. *Brain Res* **239**, 57-69.
- Lee, H.-C. and Wei, Y.-H.** (2005). Mitochondrial biogenesis and mitochondrial DNA maintenance of mammalian cells under oxidative stress. *Int J Biochem Cell Biol* **37**, 822-834.
- Li, J., Ma, X., Yu, W., Lou, Z., Mu, D., Wang, Y., Shen, B. and Qi, S.** (2012). Reperfusion promotes mitochondrial dysfunction following focal cerebral ischemia in rats. *PLoS ONE* **7**, e46498.
- Lutz, P. L. and Milton, S. L.** (2004). Negotiating brain anoxia survival in the turtle. *J Exp Biol* **207**, 3141-3147.

- Lutz, P. L. and Nilsson, G. E.** (2004). Vertebrate brains at the pilot light. *Resp Physiol Neurobiol* **141**, 285-296.
- Lutz, P. L., Nilsson, G. E. and Perez-Pinzon, M. A.** (1996). Anoxia tolerant animals from a neurobiological perspective. *Comp Biochem Physiol* **113B**, 3-13.
- Machado, B. E. and Podrabsky, J. E.** (2007). Salinity tolerance in diapausing embryos of the annual killifish *Austrofundulus limnaeus* is supported by exceptionally low water and ion permeability. *J Comp Physiol B* **177**, 809-820.
- Marchena, O. d., Guarnieri, M. and McKhann, G.** (1974). Glutathione peroxidase levels in brain. *J Neurochem* **22**, 773-776.
- Margis, R., Dunand, C., Teixeira, F. K. and Margis - Pinheiro, M.** (2008). Glutathione peroxidase family—an evolutionary overview. *FEBS Journal* **275**, 3959-3970.
- Martínez-Alvarez, R. M., Morales, A. E. and Sanz, A.** (2005). Antioxidant Defenses in Fish: Biotic and Abiotic Factors. *Rev Fish Biol Fish* **15**, 75-88.
- Masella, R., Di Benedetto, R., Vari, R., Filesi, C. and Giovannini, C.** (2005). Novel mechanisms of natural antioxidant compounds in biological systems: involvement of glutathione and glutathione-related enzymes. *J Nutr Biochem* **16**, 577-586.
- Matata, B. and Elahi, M.** (2007). Sources of reactive oxidants species in biology and disease. *Oxid Stress*, 23-38.
- Matthews, M. D., Sakmar, J. C. and Trippel, N.** (2012). Evaluation of hydrogen peroxide and temperature to control mortality caused by Saprolegniasis and to increase hatching success of Largemouth Bass eggs. *N Am J Aquacult* **74**, 463-467.
- Meister, A.** (1994). Glutathione-ascorbic acid antioxidant system in animals. *J Biol Chem* **269**, 9397-9400.
- Meller, C. L., Meller, R., Simon, R. P., Culpepper, K. M. and Podrabsky, J. E.** (2012). Cell cycle arrest associated with anoxia-induced quiescence, anoxic preconditioning, and embryonic diapause in embryos of the annual killifish *Austrofundulus limnaeus*. *J Comp Physiol B* **182**, 909-920.
- Meller, C. L. and Podrabsky, J. E.** (2013). Avoidance of apoptosis in embryonic cells of the annual killifish *Austrofundulus limnaeus* exposed to anoxia. *PLoS ONE* **8**, e75837.
- Milton, S. L., Nayak, G., Kesaraju, S., Kara, L. and Prentice, H. M.** (2007). Suppression of reactive oxygen species production enhances neuronal survival in vitro and in vivo in the anoxia - tolerant turtle *Trachemys scripta*. *J Neurochem* **101**, 993-1001.
- Mueller, S., Riedel, H.-D. and Stremmel, W.** (1997). Determination of catalase activity at physiological hydrogen peroxide concentrations. *Anal Biochem* **245**, 55-60.
- Ninfali, P. and Aluigi, G.** (1998). Variability of oxygen radical absorbance capacity (ORAC) in different animal species. *Free Radic Res* **29**, 399-408.
- Paglia, D. E. and Valentine, W. N.** (1967). Studies on the quantitative and qualitative characterization of erythrocyte glutathione peroxidase. *J Lab Clin Med* **70**, 158-169.
- Peskin, A. V. and Winterbourn, C. C.** (2000). A microtiter plate assay for superoxide dismutase using a water-soluble tetrazolium salt (WST-1). *Clin Chim Acta* **293**, 157-166.
- Peters, L. D. and Livingstone, D. R.** (1996). Antioxidant enzyme activities in embryologic and early larval stages of turbot. *J Fish Biol* **49**, 986-997.
- Plaisant, F., Clippe, A., Vander Stricht, D., Knoops, B. and Gressens, P.** (2003). Recombinant peroxiredoxin 5 protects against excitotoxic brain lesions in newborn mice. *Free Radic Biol Med* **34**, 862-872.
- Podrabsky, J., Riggs, C., Romney, A., Woll, S., Wagner, J., Culpepper, K. and Cleaver, T.** (2017). Embryonic development of the annual killifish *Austrofundulus limnaeus*: An emerging model for ecological and evolutionary developmental biology research and instruction. *Dev Dyn* **246**, 779-801.
- Podrabsky, J., Riggs, C. and Wagner, J.** (2016). Tolerance of Environmental Stress. In *Annual Fishes. Life History Strategy, Diversity, and Evolution*, eds. N. Berois G. García and R. De Sá), pp. 159-184. Boca Raton, FL USA: CRC Press, Taylor & Francis.

- Podrabsky, J. E.** (1999). Husbandry of the annual killifish *Austrofundulus limnaeus* with special emphasis on the collection and rearing of embryos. *Environ Biol Fish* **54**, 421-431.
- Podrabsky, J. E., Carpenter, J. F. and Hand, S. C.** (2001). Survival of water stress in annual fish embryos: dehydration avoidance and egg envelope amyloid fibers. *Am J Physiol* **280**, R123-R131.
- Podrabsky, J. E., Garrett, I. D. F. and Kohl, Z. F.** (2010). Alternative developmental pathways associated with diapause regulated by temperature and maternal influences in embryos of the annual killifish *Austrofundulus limnaeus*. *J Exp Biol* **213**, 3280-3288.
- Podrabsky, J. E. and Hand, S. C.** (1999). The bioenergetics of embryonic diapause in an annual killifish, *Austrofundulus limnaeus*. *J Exp Biol* **202**, 2567-2580.
- Podrabsky, J. E. and Hand, S. C.** (2000). Depression of protein synthesis during diapause in embryos of the annual killifish *Austrofundulus limnaeus*. *Physiol Biochem Zool* **73**, 799-808.
- Podrabsky, J. E. and Hand, S. C.** (2015). Physiological strategies during animal diapause: Lessons from brine shrimp and annual killifish. *J Exp Biol* **218**, 1897-1906.
- Podrabsky, J. E., Hrbek, T. and Hand, S. C.** (1998). Physical and chemical characteristics of ephemeral pond habitats in the Maracaibo basin and Llanos region of Venezuela. *Hydrobiologia* **362**, 67-78.
- Podrabsky, J. E., Lopez, J. P., Fan, T. W. M., Higashi, R. and Somero, G. N.** (2007). Extreme anoxia tolerance in embryos of the annual killifish *Austrofundulus limnaeus*: Insights from a metabolomics analysis. *J Exp Biol* **210**, 2253-2266.
- Podrabsky, J. E., Riggs, C. L. and Duerr, J. M.** (2012). Anoxia Tolerance During Vertebrate Development - Insights from Studies on the Annual Killifish *Austrofundulus limnaeus*. In *Anoxia*, (ed. P. Padilla), pp. 3-24. Rijeka, Croatia: InTech.
- Podrabsky, J. E. and Somero, G. N.** (2007). An inducible 70 kDa-class heat shock protein is constitutively expressed during early development and diapause in the annual killifish *Austrofundulus limnaeus*. *Cell Stress Chaperones* **12**, 199-204.
- Radyuk, S. N., Michalak, K., Klichko, V. I., Benes, J., Rebrin, I., Sohal, R. S. and Orr, W. C.** (2009). Peroxiredoxin 5 confers protection against oxidative stress and apoptosis and also promotes longevity in *Drosophila*. *Biochem J* **419**, 437-445.
- Rice, M. E. and Cammack, J.** (1991). Anoxia-resistant turtle brain maintains ascorbic acid content in vitro. *Neurosci Lett* **132**, 141-145.
- Rice, M. E., Lee, E. J. and Choy, Y.** (1995). High levels of ascorbic acid, not glutathione, in the CNS of anoxia - tolerant reptiles contrasted with levels in anoxia - intolerant species. *J Neurochem* **64**, 1790-1799.
- Robbins, H. M., Van Stappen, G., Sorgeloos, P., Sung, Y. Y., MacRae, T. H. and Bossier, P.** (2010). Diapause termination and development of encysted *Artemia* embryos: roles for nitric oxide and hydrogen peroxide. *J Exp Biol* **213**, 1464-1470.
- Romney, A., Davis, E., Corona, M., Wagner, J. and Podrabsky, J.** (2018). Temperature dependent vitamin D signaling regulates developmental trajectory associated with diapause in an annual killifish. *Proc Natl Acad Sci USA* **115**, 12763-12768.
- Rudneva, I.** (2013). Biomarkers for stress in fish embryos and larvae: CRC Press.
- Small, B. C. and Wolters, W. R.** (2003). Hydrogen peroxide treatment during egg incubation improves channel catfish hatching success. *N Am J Aquacult* **65**, 314-317.
- Storey, K. B.** (1996). Oxidative stress: animal adaptations in nature. *Braz J Med Biol Res* **29**, 1715-1733.
- Storey, K. B.** (2007). Anoxia tolerance in turtles: Metabolic regulation and gene expression. *Comp Biochem Physiol A Mol Integr Physiol* **147**, 263-276.
- Thannickal, V. J. and Fanburg, B. L.** (2000). Reactive oxygen species in cell signaling. *Am J Physiol Lung Cell Mol Physiol* **279**, L1005-L1028.
- Ukeda, H., Kawana, D., Maeda, S. and Sawamura, M.** (1999). Spectrophotometric assay for superoxide dismutase based on the reduction of highly water-soluble tetrazolium salts by xanthine-xanthine oxidase. *Biosci Biotechnol Biochem* **63**, 485-488.

- Valko, M., Leibfritz, D., Moncol, J., Cronin, M. T., Mazur, M. and Telser, J.** (2007). Free radicals and antioxidants in normal physiological functions and human disease. *Int J Biochem Cell Biol* **39**, 44-84.
- Wagner, E. J., Oplinger, R. W. and Bartley, M.** (2012). Effect of single or double exposures to hydrogen peroxide or iodine on salmonid egg survival and bacterial growth. *N Am J Aquacult* **74**, 84-91.
- Wagner, J., Herrejon Chavez, F. and Podrabsky, J.** (2016). Mitochondrial DNA sequence and lack of response to anoxia in the annual killifish *Austrofundulus limnaeus*. *Front Physiol* **7**, 379.
- Wagner, J., Singh, P., Romney, A., Riggs, C., Minx, P., Woll, S., Roush, J., Warren, W., Brunet, A. and Podrabsky, J.** (2018). The genome of *Austrofundulus limnaeus* offers insights into extreme vertebrate stress tolerance and embryonic development. *BMC Genomics* **19**, 155.
- Wagner, J. T. and Podrabsky, J. E.** (2015). Extreme tolerance and developmental buffering of UV-C induced DNA damage in embryos of the annual killifish *Austrofundulus limnaeus*. *J Exp Zool* **323A**, 10-30.
- Willmore, W. and Storey, K. B.** (1997). Antioxidant systems and anoxia tolerance in a freshwater turtle *Trachemys scripta elegans*. *Mol Cell Biochem* **170**, 177-185.
- Wourms, J. P.** (1972a). The developmental biology of annual fishes I. Stages in the normal development of *Austrofundulus myersi* Dahl. *J Exp Zool* **182**, 143-168.
- Wourms, J. P.** (1972b). The developmental biology of annual fishes II. Naturally occurring dispersion and reaggregation of blastomeres during the development of annual fish eggs. *J Exp Zool* **182**, 169-200.
- Wourms, J. P.** (1972c). The developmental biology of annual fishes III. Pre-embryonic and embryonic diapause of variable duration in the eggs of annual fishes. *J Exp Zool* **182**, 389-414.
- Yin, W., Signore, A. P., Iwai, M., Cao, G., Gao, Y. and Chen, J.** (2008). Rapidly increased neuronal mitochondrial biogenesis after hypoxic-ischemic brain injury. *Stroke* **39**, 3057-3063.
- Zar, J. H.** (1996). *Biostatistical Analysis*. Upper Saddle River, N.J.: Prentice Hall.
- Zelko, I. N., Mariani, T. J. and Folz, R. J.** (2002). Superoxide dismutase multigene family: a comparison of the CuZn-SOD (SOD1), Mn-SOD (SOD2), and EC-SOD (SOD3) gene structures, evolution, and expression. *Free Radic Biol Med* **33**, 337-349.
- Zhou, M., Diwu, Z., Panchuk-Voloshina, N. and Haugland, R. P.** (1997). A stable nonfluorescent derivative of resorufin for the fluorometric determination of trace hydrogen peroxide: applications in detecting the activity of phagocyte NADPH oxidase and other oxidases. *Anal Biochem* **253**, 162-168.
- Zulueta, A., Esteve, M. J. and Frígola, A.** (2009). ORAC and TEAC assays comparison to measure the antioxidant capacity of food products. *Food Chem* **114**, 310-316.

Figures

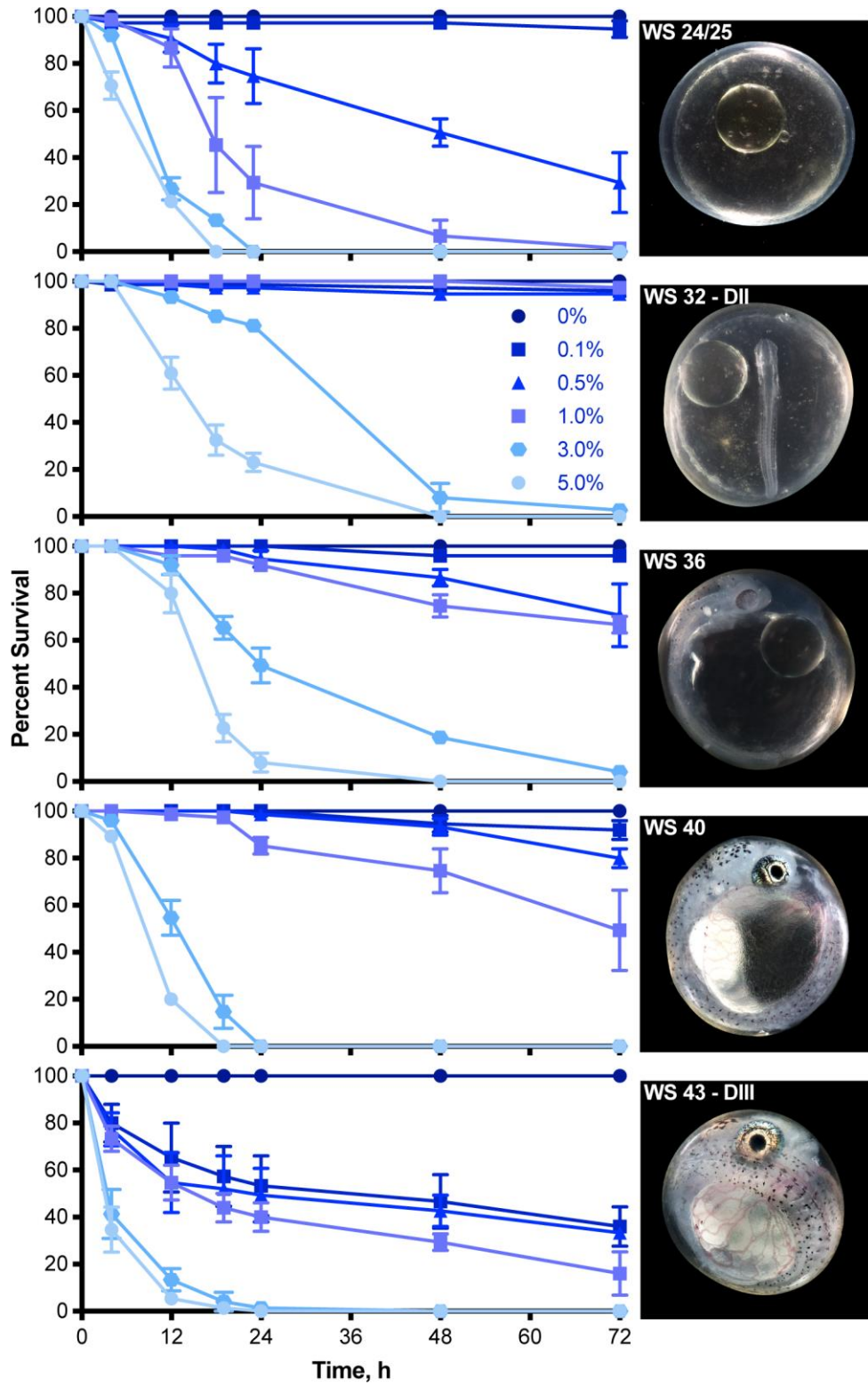


Figure 1. Survival of *Austrofundulus limnaeus* embryos exposed to continuous incubation in hydrogen peroxide. Embryos were exposed in groups of 25 starting at the developmental stage listed. Symbols are means \pm sem (n = 3).

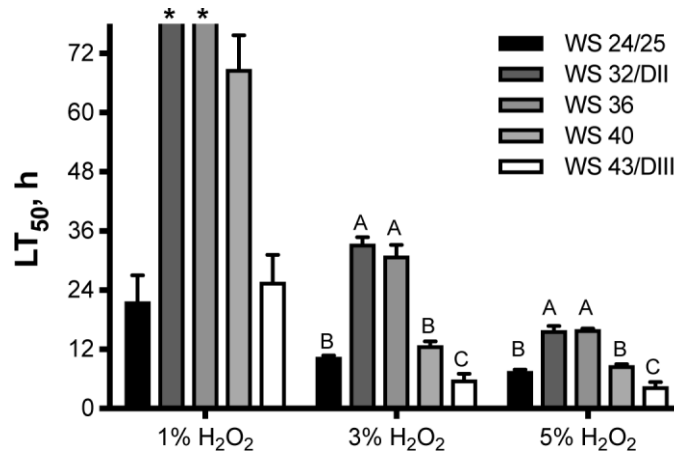


Figure 2. Lethal time to 50% mortality (LT_{50}) for *Austrofundulus limnaeus* embryos exposed continuously starting at the stage indicated to 1, 3 and 5% hydrogen peroxide.

Bars are means \pm sem ($n = 3$). Within each treatment level, bars with different letters are significantly different (ANOVA, $p < 0.001$; Tukey's MCT, $p < 0.05$). Asterisks above bars for the 1% treatment indicate no significant mortality during the 72 h trial. See images and labels in Figure 1 for information on each developmental stage.

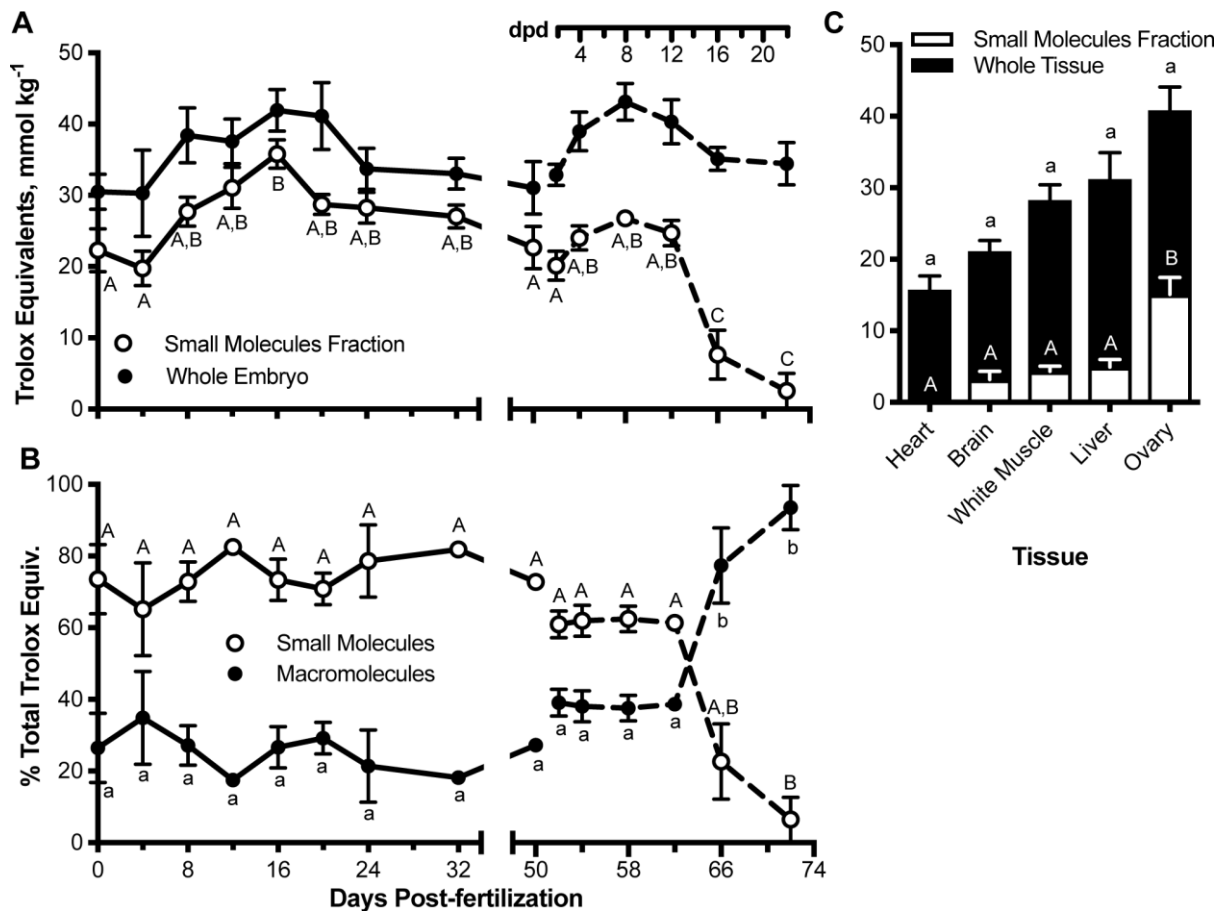


Figure 3. Oxygen radical absorbance capacity (ORAC) activity during development and in adult tissues of *Austofundulus limnaeus*. (A) Whole embryo total ORAC activity remains relatively constant across all developmental stages (one-way ANOVA, $p = 0.1$), but the amount of ORAC activity in the acid supernatant (small molecules) declines significantly during PDII development (one-way ANOVA, $p < 0.0001$). (B) There is a significant shift in the percentage of the whole embryo total ORAC activity that is due to small molecules (acid supernatant) compared to macromolecules (acid precipitate) during PDII development (one-way ANOVA, $p < 0.0001$). Symbols are means \pm SEM ($n = 3$). Solid lines denote early development through diapause II, while dashed lines indicate PDII development. Symbols with different letters are statistically different (one-way ANOVA with Tukey's MCT, $p < 0.05$). (C) Total and small molecule ORAC activity for adult female tissues of *A. limnaeus*. Note that only ovary tissue has a

large contribution of small molecules to the total ORAC activity. Bars are means \pm sem (n = 4). dpd, days post-diapause II. Bars with different letters are statistically different (one-way ANOVA with Tukey's MCT, $p < 0.05$). Statistical comparisons were made separately among the whole tissue and small molecule fractions between tissues, but whole tissue and supernatant values were not compared within a tissue. For the whole adult tissue data there was a significant trend in ORAC activity between tissues (ANOVA, $p = 0.04$), but *post hoc* tests were unable to statistically distinguish individual means.

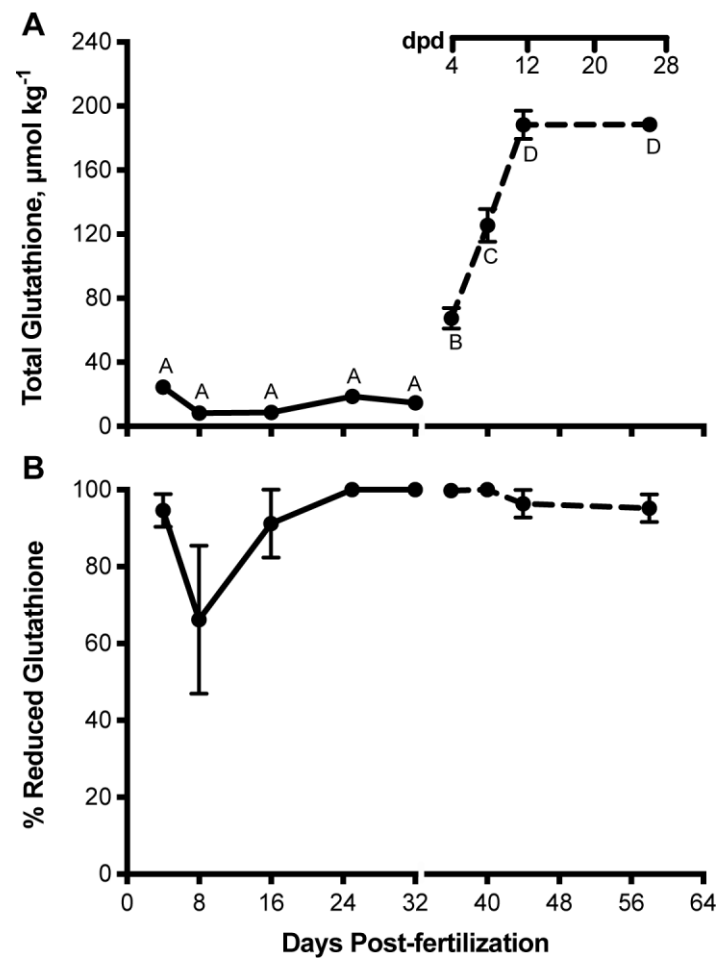


Figure 4. Total glutathione levels increase during post-diapause II development while the percent reduced glutathione remains stable in *Austrofundulus limnaeus* embryos. (A)

Total glutathione levels increase significantly after embryos break diapause II. Symbols with different letters are statistically different, (Tukey's MCT, $p < 0.001$). Solid lines connect data from early development through diapause II, while dashed lines connect data from PDII embryos. **(B)** The percent of the total glutathione pool that was reduced did not change significantly during development (one-way ANOVA, $p = 0.08$). Symbols are means \pm sem; ($n=4$). dpd, days post-diapause II.

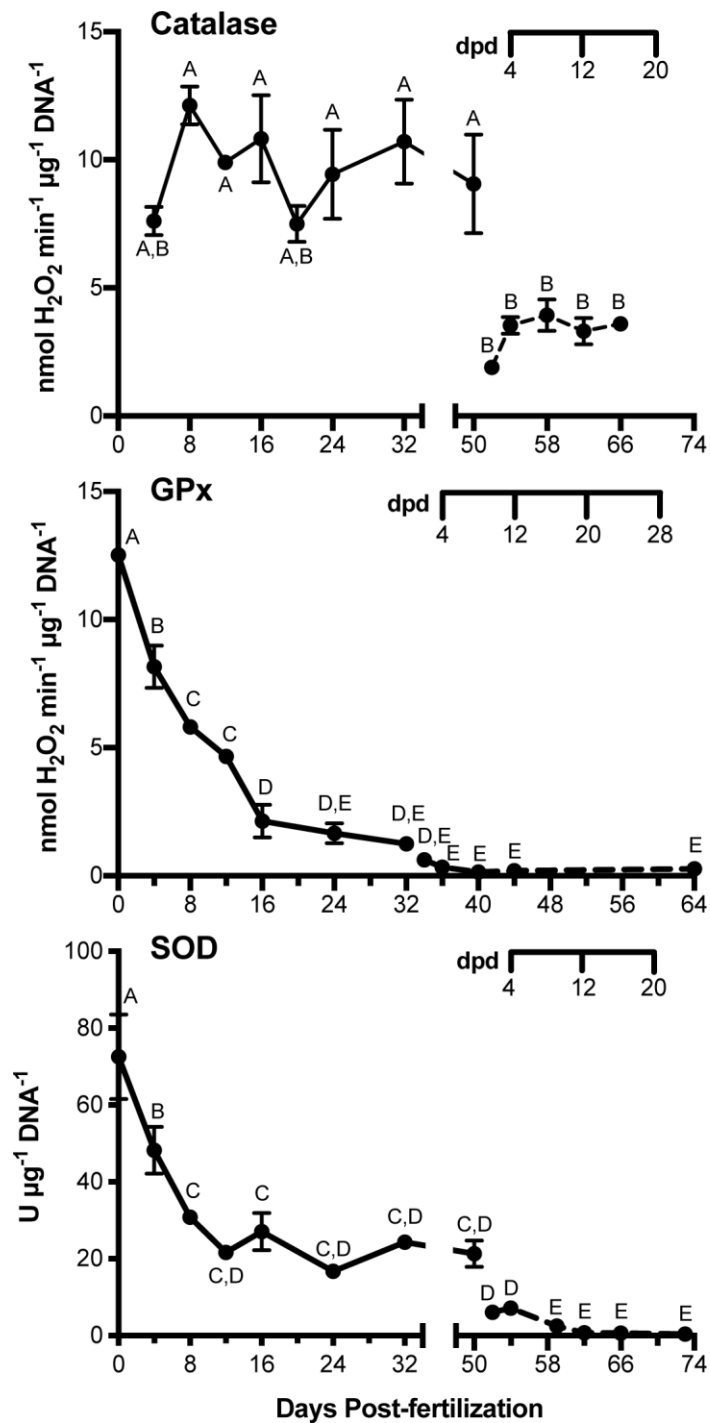


Figure 5. Total activity of catalase, SOD, and GPx in *Austrofundulus limnaeus* embryos is dynamic across development. When the data are normalized to total DNA content (a proxy for cell number during development), enzymatic capacity is greatest in early development for all three enzymes. Within each graph, symbols with different letters are statistically different (one-

way ANOVA, Tukey's MCT, $p < 0.05$). Symbols are means \pm sem ($n = 4$ for SOD and GPx; $n = 3$ for catalase). dpd, days post-diapause II.

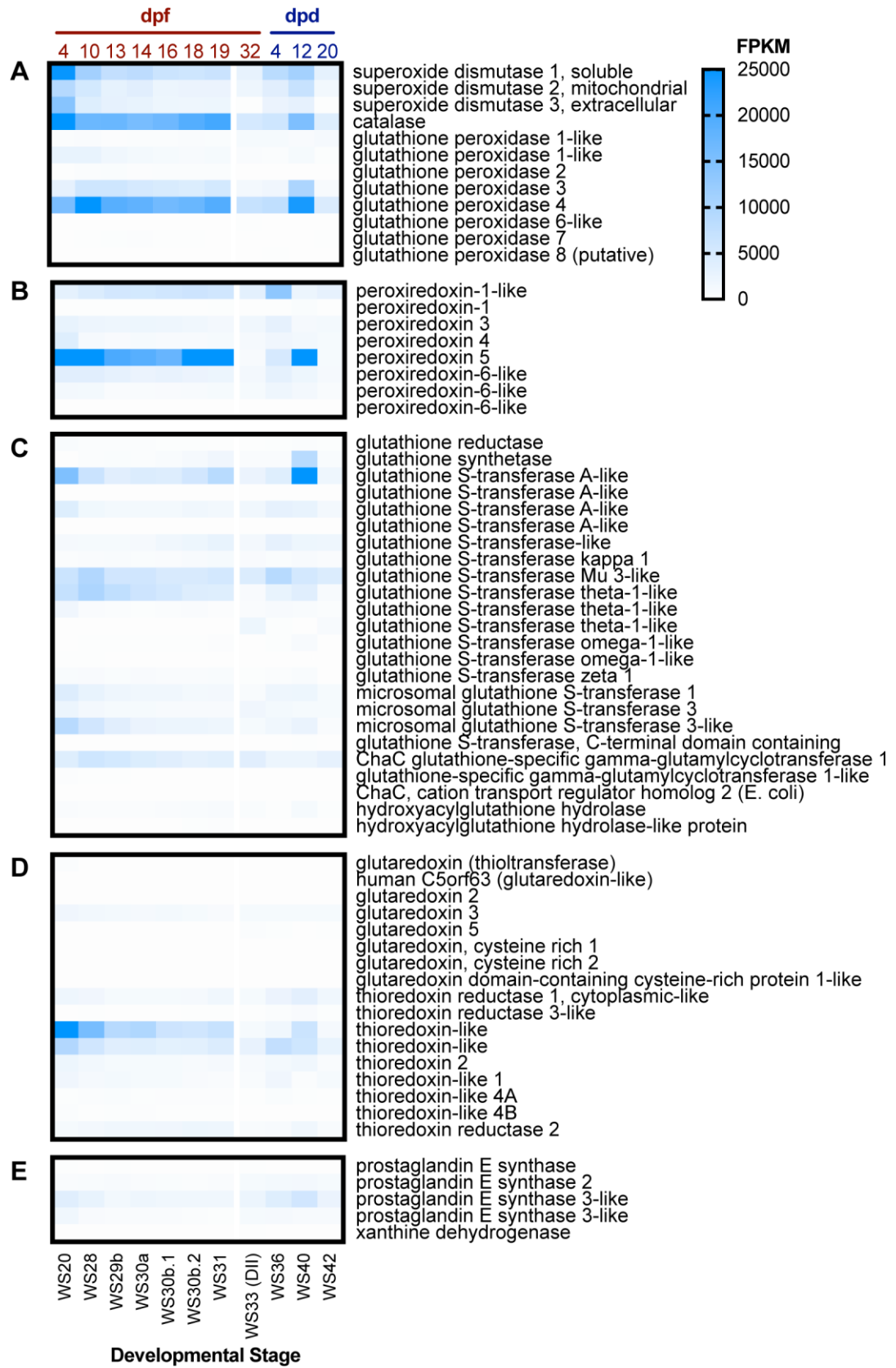


Figure 6. Transcript levels for common antioxidant enzyme systems in *Austrofundulus*

***limnaeus* as determined by RNA sequencing.** Enzyme systems are organized into groups: **(A)** superoxide dismutase, catalase, and glutathione peroxidase isoforms, **(B)** peroxiredoxins, **(C)** glutathione metabolism, **(D)** glutaredoxin and thioredoxin systems, and **(E)** miscellaneous. Data for pre-diapause II development (WS 20-31) were incubated at 20°C and were collected at the developmental stages listed at the bottom of the heat map. Time to reach these stages at 25°C are listed at the top of the heat map and were determined based on Podrabsky et al. (2017). Embryos in DII and PDII stages were incubated at 25°C. Expression levels are reported as mean fragments per kilobase per million reads mapped (FPKM). For pre-diapause II stages, n = 3 (Romney et al., 2018). For DII and PDII stages, n=4-6 (Wagner et al., 2018).

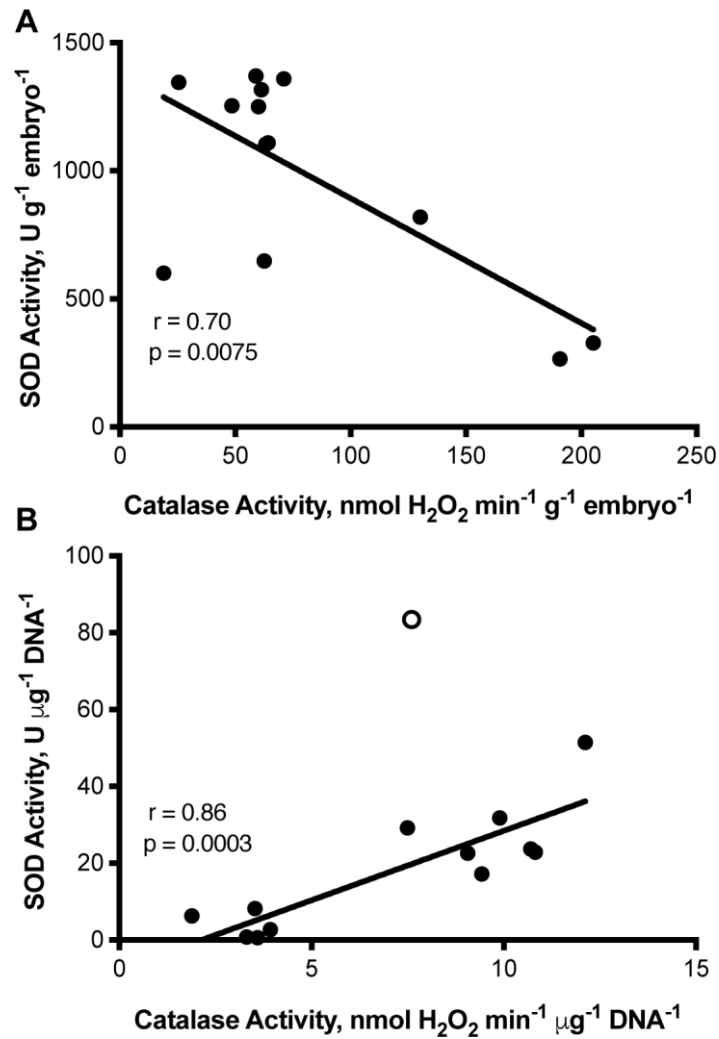


Figure 7. Total catalase and SOD activity are correlated across *Austrofundulus limnaeus* development. Activity is expressed (A) per g embryo, or (B) per μg DNA. Each data point is a single embryonic stage. Activity levels and embryonic stages are based on the same dataset as Figure 5. The open circle in panel B (0 dpf embryos) is a statistical outlier and was not included in the linear regression (Prism 7.0 ROUT, Q = 5%). Mean activities for each developmental stage are plotted (n = 4 for SOD; n = 3 for catalase).

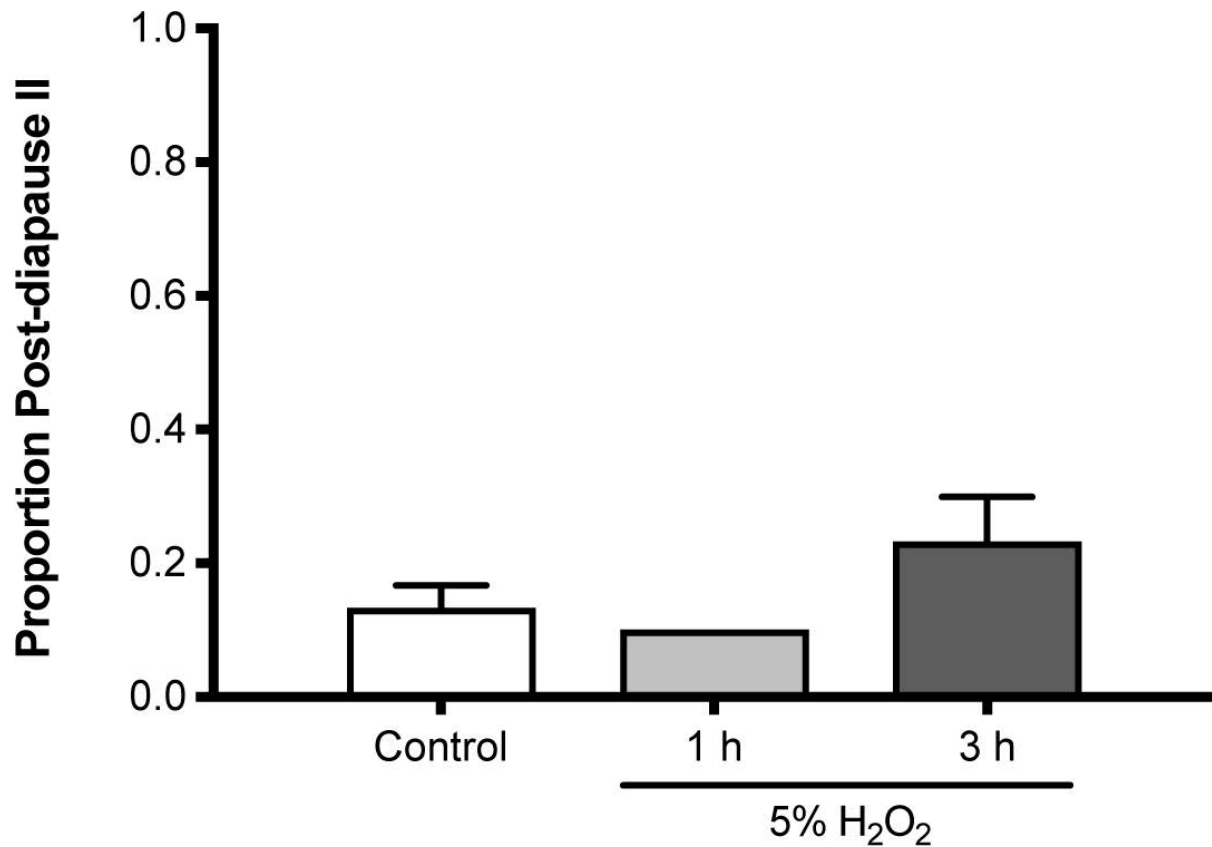


Figure S1. Proportion of *A. limnaeus* DII embryos that exited diapause following H₂O₂ exposure. Embryos were monitored for 11 days following H₂O₂ exposure for the resumption of embryonic development. Exposed embryos did not exit diapause II at a higher frequency than unexposed controls (one-way ANOVA, $p = 0.166$). Bars are means \pm sem ($n=3$).

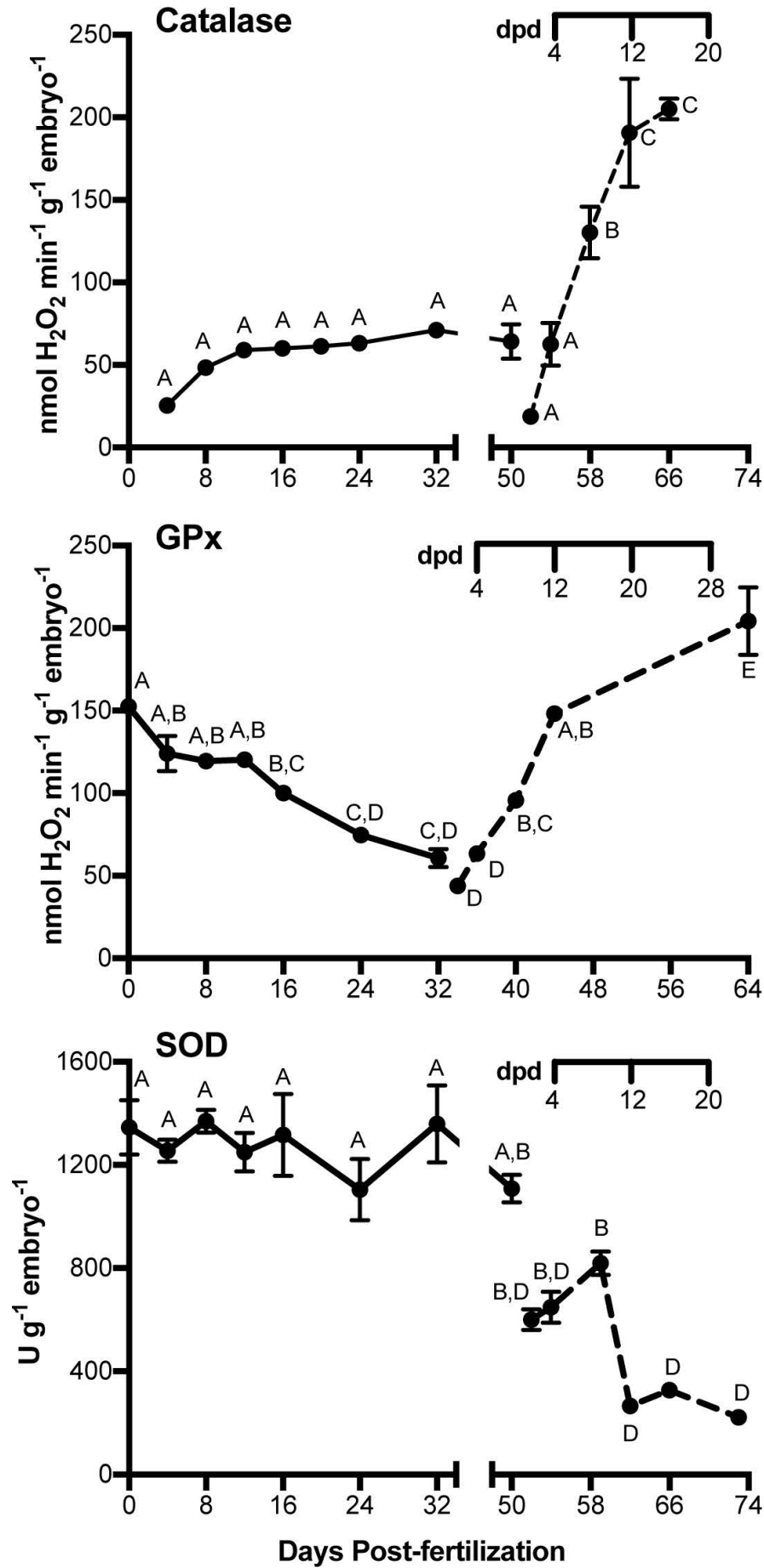


Figure S2. Antioxidant enzyme capacity expressed per g embryo. When expressed by per g of embryo, enzyme activities of all three antioxidant enzymes showed unique profiles during *A. limnaeus* development. Catalase activity from whole embryo homogenates remained relatively constant in early development through DII. However, a significant increase occurred during post-diapause II development with activity reaching over 200 nmol H₂O₂ min⁻¹ g⁻¹ at 16 dpd (one-way ANOVA with Tukey's MCT, $p < 0.05$). In contrast, SOD activity remained high and relatively constant through early development and DII. During post-diapause II development, SOD activity dropped, and further declined to its lowest levels below 400 U g⁻¹embryo by 12 dpd. GPx activity steadily declined during embryonic development and reaches its lowest activity levels during DII. During post-diapause II development, GPx activity increased steadily and reached its highest activity levels at the end of embryonic development (one-way ANOVA with Tukey's MCT, $p < 0.05$).

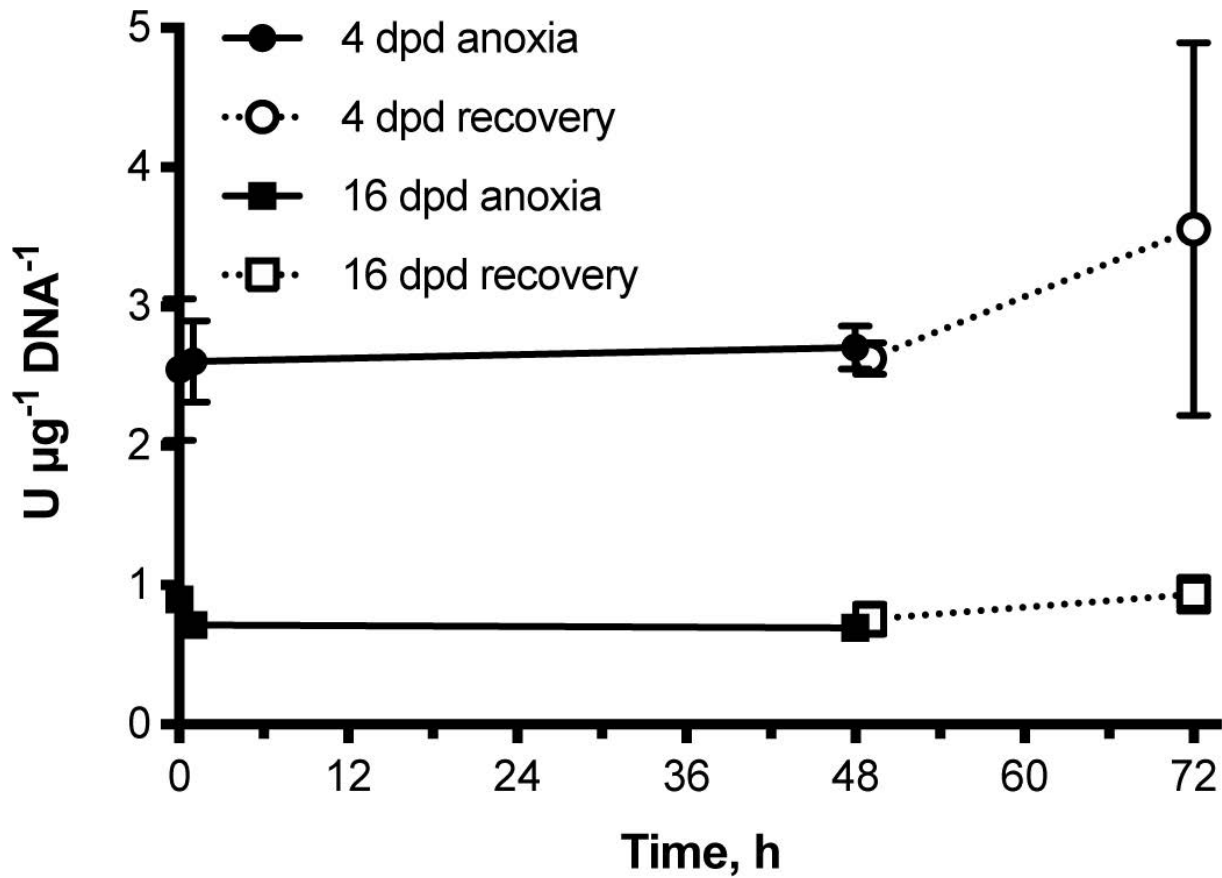


Figure S3. Total SOD activity expressed per µg of DNA remains stable during anoxia and recovery from anoxia. Symbols are means ± sem (n=3). Closed symbols with solid lines represent time in anoxia, while open symbols and dotted lines represent time in aerobic recovery from anoxia.